

1 **Comparison of On-Line and Off-Line Methods to Quantify**
2 **Reactive Oxygen Species (ROS) in Atmospheric Aerosols**

3

4 S. J. Fuller, F. P. H. Wragg, J. Nutter, M. Kalberer*

5

6

7 Department of Chemistry, University of Cambridge, Lensfield Road, Cambridge
8 CB2 1EW, UK

9

10 * Corresponding author:

11 Email: markus.kalberer@atm.ch.cam.ac.uk

12 Tel: 0044 1223 336392

13 Fax: 0044 1223 336362

14

15

16 **Abstract**

17 Atmospheric aerosol particle concentrations have been linked with a wide range
18 of pulmonary and cardio-vascular diseases but the particle properties
19 responsible for these negative health effects are largely unknown. It is often
20 speculated that reactive oxygen species (ROS) present in atmospheric particles
21 lead to oxidative stress in, and ultimately disease of, the human lung. The
22 quantification of ROS is highly challenging because some ROS components such
23 as radicals are highly reactive and therefore short-lived. Thus, fast analysis
24 methods are likely advantageous over methods with a long delay between
25 aerosol sampling and ROS analysis. We present for the first time a detailed
26 comparison of conventional off-line and fast on-line methods to quantify ROS in
27 organic aerosols. For this comparison a new and fast on-line instrument was
28 built and characterized to quantify ROS in aerosol particles with high sensitivity
29 and a limit of detection of 4 nmol H₂O₂ equivalents per m³ air. ROS
30 concentrations are measured with a time resolution of approximately 15
31 minutes, which allows the tracking of fast changing atmospheric conditions. The
32 comparison of the off-line and on-line method shows that, in oxidized organic
33 model aerosol particles, the majority of ROS have a very short lifetime of a few
34 minutes whereas a small fraction is stable for a day or longer. This indicates that
35 off-line techniques, where there is often a delay of hours to days between
36 particle collection and ROS analysis, may severely underestimate true ROS
37 concentrations and that fast on-line techniques are necessary for a reliable ROS
38 quantification in atmospheric aerosol particles and a meaningful correlation
39 with health outcomes.

40

41 **Keywords:** organic aerosol; health effects; on-line analysis

42

43

44 **1 Introduction**

45 Aerosol particles have long been associated with adverse health effects in the
46 population (Dockery et al., 1993) and are a major public health issue. High
47 atmospheric particle concentrations have been linked in epidemiological studies
48 with e.g., asthma, chronic obstructive pulmonary disease, cardio vascular

49 diseases and overall mortality (Brunekreef and Holgate, 2002). Many efforts
50 have been made to link these health effects to specific aerosol properties. Studies
51 have focused on physical particle properties such as mass, number concentration
52 and surface area as well as on the metal fraction or on specific organic
53 compounds such as polycyclic aromatic hydrocarbons but so far no particle
54 property could be clearly and consistently linked with the above-mentioned
55 health effects (de Kok et al., 2006, Gerlofs-Nijland et al. 2007). Potential links
56 between the organic fraction of aerosol particles and health effects have hardly
57 been investigated. This may be in part due to the complexity of the organic
58 particle composition and the subsequent poor understanding of which
59 components might be most relevant for the organic fraction's health impact, and
60 in part due to the lack of continuous long-term records of organic aerosol
61 particle composition. The organic fraction often makes up more than 50 % of the
62 aerosol mass and therefore a more detailed analysis of health-relevant organic
63 particle properties is urgently needed.

64

65 Many studies hypothesise that oxidizing components in aerosol particles cause
66 oxidative stress in the lung, which may eventually lead to inflammation and
67 disease (Dellinger et al., 2001; Donaldson et al., 2003; MacNee and Donaldson,
68 2003). Oxidative stress is defined here as a disturbance in the pro-oxidant (i.e.,
69 aerosol component) – anti-oxidant balance in favour of the former leading to
70 potential biomolecular damage (Halliwell and Gutteridge, 2007). Particle
71 components which cause oxidative stress are often defined as Reactive Oxygen
72 Species (ROS), and potentially include a wide range of inorganic and organic
73 compounds such as transition metals, hydrogen peroxide (H_2O_2), radicals (e.g.,
74 OH^\bullet , $O_2^{\bullet-}$), and organic (hydro-) peroxides. A number of studies have linked ROS
75 present in organic aerosol to observed health effects (e.g., Pryor and Church,
76 1991, Donaldson et al., 2003).

77

78 There have been many studies that use adapted biological assays to study the
79 ROS concentration of ambient and laboratory generated aerosol. One of the most
80 popular assays uses the fluorescence probe 2',7'-dichlorofluorescein (DCFH),
81 which is reactive to a range of ROS and, which is used in combination with

82 horseradish peroxidase (HRP). HRP is a redox enzyme that reacts mainly with
83 hydrogen peroxide and organic hydroperoxides (Berglund et al., 2002;
84 Furtmüller et al., 2000; Cathcart et al., 1983). The reactivity of HRP towards
85 other ROS is not very well described but a range of ROS components such as
86 Criegee radicals and peroxy radicals can form hydrogenperoxides in an aqueous
87 solution (Pryor and Church, 1991; Wang et al., 2012; Hasson et al., 2001) and can
88 thus be quantified indirectly with the DCFH/HRP assay.

89

90 ROS are usually quantified with off-line techniques in extracts of aerosol
91 particles collected on filters (Hung and Wang, 2001; Venkatachari et al., 2005).
92 Due to the reactive nature of ROS, such off-line methods risk severely
93 underestimating the true ROS concentration in particles because some ROS
94 components (e.g., radicals or peroxides) might decompose during sample
95 collection and work-up. Therefore, two recent studies presented on-line and
96 semi on-line techniques to quantify particle-bound ROS with DCFH with the aim
97 to reduce the time between collection and analysis associated with filter
98 collection and for higher time resolution measurements (Wang et al., 2011; King
99 and Weber, 2013).

100

101 In this study we present a new on-line instrument further developing the
102 concept of Wang et al. (2011) that uses a continuous flow version of the
103 DCFH/HRP assay for the quantification of particle-bound ROS. The instrument is
104 designed to allow for a very gentle and fast ROS extraction to minimize ROS
105 decomposition before analysis. We present a characterisation of the instrument
106 performance and present for the first time a detailed comparison between off-
107 line filter collection methods and the on-line automated system for ROS
108 quantification to establish the advantages of on-line measurements. Results
109 clearly show that the major fraction of ROS in oxidized organic aerosol particles
110 has a very short lifetime emphasizing the need for fast on-line ROS analysis
111 techniques.

112

113

114 **2 Experimental**

115 At the core of the instrument described here is the aqueous phase reaction cycle
116 of ROS with horseradish peroxidase (HRP) and 2'7'-dichlorofluorescein (DCFH)
117 leading to the fluorescent reaction product DCF, which is ultimately quantified
118 and related to the ROS concentration in the aerosol particles. The general
119 reaction mechanism between ROS, HRP and DCFH is described below. This is
120 followed by a description of the model aerosol particle generation, the new on-
121 line instrument, a corresponding off-line method, and the comparison between
122 these two methods.

123

124 **2.1 DCFH Assay**

125 Liquid phase ROS concentrations were quantified using the fluorescence probe
126 DCFH in combination with the peroxidase enzyme catalyst HRP. As shown in
127 Figure 1a, H₂O₂ (also representing other ROS) reacts with HRP to form an
128 intermediate which subsequently oxidises two equivalents of DCFH to the
129 fluorescent product DCF (Berglund et al., 2002). The concentration of the
130 product DCF is measured using fluorescence spectroscopy (excitation at 470 nm
131 and emission at 520 nm). HRP is reactive towards hydrogen peroxide, organic
132 hydroperoxides (Cathcart et al., 1983) and, as mentioned above, possibly other
133 ROS components as part of the peroxidase cycle.

134

135 Background steady state concentrations of H₂O₂ at concentration levels of up to
136 60 nmol dm⁻³ are present in laboratory grade deionised water as it is in
137 equilibrium with dissolved oxygen giving rise to an unavoidable background
138 fluorescence signal (Hwang and Dasgupta, 1986; Venkatachari and Hopke,
139 2008). In addition, dissolved oxygen can also react with HRP to oxidise DCFH to
140 DCF in the oxidase cycle as shown in Figure 1b. Both the background
141 concentrations of H₂O₂ and reaction with oxygen can be accounted for by the
142 subtraction of blank measurements. Previous studies have attempted to reduce
143 the background by removal of H₂O₂ using metal catalysts such as MnO, however,
144 once removed, steady state concentrations of H₂O₂ re-establish rapidly, a process
145 which is accelerated by visible and long wave UV light (Venkatachari and Hopke,
146 2008). To reduce the variability in background H₂O₂ concentrations, and to
147 prevent photo-oxidation of DCFH, the assay was carried out under dark

148 conditions. H₂O₂ concentrations in the blank are in the same order of magnitude
149 as the ROS in aerosol particles (see below). Thus, a careful characterisation and
150 subtraction of the blank, especially its stability over time, is necessary for
151 reliable results. In this study the assay is calibrated using H₂O₂ and all results are
152 given as an equivalent H₂O₂ concentration.

153

154 The fluorescent probe DCFH is very reactive and prone to decomposition and is
155 therefore synthesised each day it is used. It is synthesised from the stable di-
156 acetate form DCFH-DA. For a 250 ml 10 μM DCFH solution, a stock solution of
157 DCFH-DA (Sigma Aldrich) in methanol (1.218 ml, 1.0 mg ml⁻¹) is reacted with
158 sodium hydroxide (10 ml, 0.01 mol dm⁻³) for 30 min under dark conditions. To
159 make a pH 7.2 buffered solution and neutralise any remaining sodium hydroxide,
160 phosphate buffered saline (PBS) (Sigma Aldrich) is added (25 ml, 1.0 mol dm⁻³)
161 to make a final solution of 10 μmol dm⁻³ DCFH in 0.1 mol dm⁻³ PBS. Horseradish
162 peroxidase (HRP) (Type VI, Sigma Aldrich) solutions are made up in HPLC water
163 (Rathburn) and 10 % PBS.

164 The DCF detection system is described below in 2.3 and 2.4.

165

166 **2.2 Aerosol Generation**

167 Oleic acid aerosol particles were generated and oxidized using the apparatus
168 shown in Figure 2. To characterize the instrument developed here oxidized oleic
169 acid was chosen as a model of aged organic aerosol which has been well
170 characterised in earlier studies (Vesna et al., 2009; Ziemann, 2005). Oleic acid
171 particles are ideal for such a calibration because the oxidation products are
172 reasonably well understood and include a range of different functional groups
173 that reflect potentially health-relevant compound classes present in atmospheric
174 aerosol. This specifically includes peroxides, hydroperoxides, stabilized Criegee
175 radical intermediates, as well as organic acids and aldehydes (Ziemann, 2005).

176

177 Oleic acid aerosol particles were generated by heating approximately 2.0 ml of
178 pure oleic acid (Reagent Grade 99 %, Sigma Aldrich) in a schlenk flask contained
179 in a heated aluminium block (100-110°C) (Figure 2). Nitrogen was flowed
180 through the flask at 0.5 L min⁻¹. Oleic acid particles were formed through

181 homogenous nucleation downstream of the flask as the vapour cooled to room
182 temperature. Ozone gas was generated by flowing air, at 1 L min⁻¹, past a 185 nm
183 UV light source (Appleton Woods). To simulate aged (oxidized) aerosol particles
184 the ozone and particle flows were combined and passed through a 2 L glass tube,
185 giving a reaction time of approximately 80 seconds, and an ozone concentration
186 of 130 ppm. The ozone concentration was measured using a commercial ozone
187 analyzer (49i, Thermo Scientific). The oxidized aerosol was then passed through
188 an activated charcoal denuder to remove excess ozone and organic vapours.
189 Ozone concentrations were regularly measured after the denuder to assure that
190 all ozone was removed by the denuder. Then the aerosol was diluted with
191 nitrogen to make a total flow of 6 L min⁻¹. Experiments were carried out at room
192 temperature (~ 20 °C) and at low relative humidity (< 2 % RH).

193

194 Particle size distributions were measured using a Scanning Mobility Particle
195 Sizer (SMPS): a TSI model 3081 differential mobility analyser (DMA) combined
196 with a model 3775 condensation particle counter (CPC). The SMPS operated at a
197 sampling rate of 0.3 L min⁻¹ and a DMA sheath flow of 3 L min⁻¹ giving a
198 measurable particle size range of 14 – 700 nm. Particle number size distribution
199 data was acquired using TSI AIM software. The density of the oxidized particles
200 was assumed to be 1.0 g cm⁻³ as taken from previous studies of oxidised organic
201 acid particles (Katrib et al., 2005).

202

203 Aerosol mass concentrations were controlled through the oleic acid heating
204 temperature. The temperature was varied between 100 – 110 °C and could be
205 maintained with a variability of ± 0.5 °C. This corresponded to a stable and
206 adjustable oleic acid aerosol particle mass concentrations of 10 – 200 µg m⁻³ with
207 a variability of typically less than ± 10 % over a period of 1 hour and with a
208 particle size mode of 93 ± 5 nm throughout the entire mass range.

209

210 **2.3 On-line Measurements**

211 Figure 3 shows a schematic of the on-line instrument for ROS quantification,
212 which combines in a continuous flow system an efficient particle collection with
213 the DCFH/HRP assay described above.

214

215 Air is pumped through the particle collector (Takeuchi et al., 2005) at a flow rate
216 of 5 L min^{-1} where it intersects with the aqueous HRP collection solution (1 unit
217 ml^{-1} , 10 % PBS) pumped at 1 ml min^{-1} using a peristaltic pump (Watson Marlow
218 323 with 318C pump head) . This creates a fine spray of the collection solution.
219 The spray serves two functions: to uniformly wet the filters used for collection of
220 particles and to allow direct collection of particles through collision with the
221 spray droplets within a fraction of a second of entering the instrument. If not
222 collected in the spray, particles come into contact with the HRP solution on the
223 filters and their water-soluble fraction is extracted into the solution where ROS
224 can react with HRP. Therefore it is difficult to define an exact time between
225 particles entering the instrument and the reaction of extracted ROS components
226 with HRP but due to the compact design of the particle collector it is estimated
227 that this is on a time scale of seconds to a few minutes. The filters consist of a
228 paper filter (25 mm, Whatman Type 1) on top of a hydrophilic support filter (25
229 mm, Millipore, Isopore™, $5.0 \mu\text{m}$). The collection efficiency is greater than 95 % for
230 particles with an aerodynamic diameter $> 100 \text{ nm}$, and drops to 50 % at 50 nm.
231 The solution is collected in the base of the particle collector, from where it is
232 pumped out at 1 ml min^{-1} . The particle extract/HRP solution is then mixed with
233 DCFH solution ($10 \mu\text{mol L}^{-1}$, 10 % PBS) also being pumped at 1 ml min^{-1} . This
234 mixing dilutes both reactants to the same concentrations of HRP (0.5 unit ml^{-1})
235 and DCFH ($5 \mu\text{mol L}^{-1}$) used in the off-line method described later.

236 The effect of HRP concentrations higher than 0.5 unit ml^{-1} was tested. While this
237 resulted in an increased reaction rate with ROS it also increased the background
238 reactions described in Figure 1b and thus did not result in an overall better
239 sensitivity of the assay.

240 The combined solution then flows through a 20 ml Teflon tubing (3.175 mm OD,
241 1.5 mm ID) reaction coil, immersed in a water bath at 40°C , giving a reaction
242 time of approximately 10 minutes in the water bath. The total residence time of
243 the reagents in the flow system (from the point of mixing to the fluorescence
244 measurement) is approximately 15 minutes, shown in off-line studies to allow
245 for complete reaction of the assay with H_2O_2 concentrations up to 800 nmol dm^{-3}
246 (as shown later, Figure 6a). The solution is then passed through a quartz

247 fluorescence flow cell with a 1 cm² cross-section and a 3 cm³ volume. Due to
248 inhomogeneous mixing, the mixing time in the fluorescence flow cell is
249 approximately 15 minutes, limiting the time resolution of measurements. The
250 cell is mounted vertically, with the solution entering at the base, allowing for gas
251 bubbles in the system to rise quickly to the top of the cell without affecting
252 fluorescence measurements. The fluorescence is measured using a temperature
253 stabilised LED light source (470 nm, Luxeon V Star) coupled with an Ocean
254 Optics USB2000+ spectrometer recording the fluorescence emission of DCF at
255 520 nm. The fluorescence data is acquired and analysed using LabView (National
256 Instruments, version 8.6). Between successive measurements the instrument can
257 be cleaned by replacing the aerosol flow with a clean flow of synthetic air till ROS
258 concentrations reach blank levels.

259

260 This on-line instrument differs from previously described instruments mainly in
261 the particle collection process. The only other on-line instrument described in
262 the literature (Venkatachari and Hopke, 2008; Wang et al., 2011) uses a particle
263 into liquid sampler (PILS)(Orsini et al., 2003), which allows particle collection at
264 high flow rates (15 L min⁻¹) but uses a high temperature steam to grow particles
265 for collection: these high temperatures may influence analysis of the sample due
266 to the unstable nature of some ROS. In the instrument described in this study,
267 ROS-containing particles are mixed and extracted with the HRP solution at room
268 temperature.

269 In another system recently described (King and Weber, 2013) samples are
270 collected for a time period of five minutes before analysis using the DCFH/HRP
271 assay. This short delay of five minutes before analysis may lead to loss of reactive
272 components (see comparison of on-line and off-line method below).

273

274 **2.4 Off-line Measurements**

275 Off-line measurements of the fluorescence response of the DCFH/HRP assay with
276 H₂O₂ were used to optimize operation conditions of the on-line instrument and
277 to compare the performance of on-line and off-line quantification methods.
278 Solutions of known H₂O₂ concentration (0.8 ml) were combined with DCFH (1 ml,
279 10 μM, 20 % PBS) and HRP solution (0.2 ml, 5 unit ml⁻¹) in a disposable UV-

280 cuvette (Brand, semi-micro, Sigma Aldrich), giving final concentrations of HRP
281 and DCFH as used in the on-line measurements. Fluorescence measurements
282 were taken continuously during a 15-minute reaction time using a 4-way cuvette
283 holder (Ocean Optics), which was maintained at 40 °C by passing heated water
284 through its base. The 15-minute reaction time allows for complete reaction (see
285 discussion below and Figure 6a) and is equivalent of the reaction time in the on-
286 line instrument. The same light source, spectrometer, and software were used as
287 for the on-line method.

288

289 In addition to H₂O₂ calibration solutions, ROS concentrations were also
290 quantified in oxidized oleic acid particles with the off-line method and compared
291 with the on-line instrument. For this comparison aerosol samples were collected
292 on Teflon filters (Millipore, Durapore, 0.1 µm, 47 mm, Sigma Aldrich) at a flow rate
293 of 5 L min⁻¹. The filters were collected for a range of times from 1 – 15 minutes.
294 To determine the total particle mass on the filters the aerosol size distribution at
295 the time of collection was measured using a SMPS, with a typical mass concentration
296 of 100 - 200 µg m⁻³. Following collection, a 14 mm diameter punch of the filter
297 was extracted in water (1 ml, HPLC grade, Rathburn). Two different methods
298 were compared for extraction, firstly sonication for 15 minutes in an ultrasonic
299 bath (Grant), and secondly vortexing for 3 minutes in a vortex mixer (Fisher-
300 Scientific). The 3-minute time for vortexing was established as the time for
301 maximum yield whilst analysing the samples as fast as possible. The aqueous extract
302 (0.8 ml) was combined with DCFH (1ml, 10 µM, 20 % PBS) and HRP solution (0.2
303 ml, 5 unit ml⁻¹) in a disposable UV cuvette and analysed as described above for
304 H₂O₂ calibration solutions. Blank filter measurements were taken for each
305 particle collection time by placing a HEPA filter in front of the collection filter
306 and these were subtracted from the equivalent sample measurements.

307

308

309 **3 Results and Discussion**

310

311 **3.1 Online Measurements**

312 The sensitivity of the on-line instrument was determined with H₂O₂ standard
313 calibration solutions. For this the particle collector was by-passed and reactants
314 were pumped directly out of their respective reservoirs to the heated reaction
315 coil. Known H₂O₂ concentrations were included in the DCFH stock for calibration
316 as this mixture is un-reactive without HRP. The fluorescence of the reaction
317 mixture was measured after a 15-minute reaction time. Concentrations of
318 reactants in the flow system were as described above (i.e., 0.5 unit ml⁻¹ and 5
319 μmol dm⁻³ for HRP and DCFH, respectively). The calibration results are shown in
320 Figure 4, showing a strong linear relationship between the fluorescence intensity
321 and H₂O₂ concentration up to 200 nmol dm⁻³. The limit of detection (LOD) of
322 H₂O₂ in the liquid phase is approximately 10 nmol dm⁻³ and is derived from the
323 variability (three standard deviations) of the blank signal intensity, taken on the
324 same day. Absolute fluorescence intensities of the blank were approximately
325 2000 counts and the data shown in Figure 4 is blank subtracted. Blank
326 measurements of the solvent are taken at least once a day. This LOD equates to
327 an aerosol phase LOD of approximately 4 nmol H₂O₂ m⁻³, based on a particle
328 extract/HRP flow rate of 1 ml min⁻¹, a gas sampling rate through the particle
329 collector of 5 L min⁻¹ and a flow system liquid flow rate of 2 ml min⁻¹ with a
330 linear range from 4 to at least 80-100 nmol H₂O₂ m⁻³. This detection limit should
331 be sufficient for ambient atmosphere measurements where often ROS
332 concentrations of around 5 nmol m⁻³ were reported (Venkatachari et al., 2005;
333 Wang et al., 2011 and references therein). King and Weber (2013) measured
334 lower ROS concentrations with an average of 0.16 nmol H₂O₂ m⁻³, which would
335 be below the LOD of our current instrument version.

336 The ROS concentrations detected and reported below for the oxidized oleic acid
337 aerosol particles are given as equivalent H₂O₂ concentrations.

338

339 To characterize the instrument further, and with real aerosol particles, the ROS
340 concentration was quantified in oxidized oleic acid particles. Oleic acid particles
341 were generated as described above and particle-bound ROS concentrations were
342 measured over a range of aerosol mass concentrations (10 – 170 μg m⁻³) to
343 generate a calibration curve including the particle collector and thus assessing
344 the linearity of the instrument response considering all parts of the on-line

345 instrument. The particle size distribution was measured using an SMPS and the
346 modal size (93 ± 5 nm) was found not to change for the mass concentrations
347 range considered here. Comparison of the collection efficiency of the particle
348 collector with the generated aerosol size distribution showed that the particle
349 collector was able to sample more than 90 % of the aerosol mass.

350

351 On-line measurements shown in Figure 5 were taken over three separate days
352 and only small day-to-day variation was observed. Blank measurements, taken
353 by placing a HEPA filter in front of the particle collector, were subtracted from
354 sample measurements. The aerosol generation technique was repeatable and
355 generated particles with a consistent ROS concentration per particle mass for a
356 wide range of mass concentrations. Thus, oxidized oleic acid can be used as a
357 true, easy to use, and reliable aerosol standard for ROS.

358

359 A strong correlation between the total particle mass and the ROS concentration
360 is observed (Figure 5). The linear range of the aerosol calibration extends over a
361 similar range as the calibration with H_2O_2 standard solutions shown in Figure 4,
362 i.e., from ~ 20 to ≥ 100 $\text{nmol H}_2\text{O}_2 \text{ m}^{-3}$. If a linear fit is applied to the data, the
363 gradient indicates a concentration of 0.58 ± 0.07 nmol ROS (i.e., H_2O_2
364 equivalents) per μg of oxidized oleic acid particle mass.

365

366 **3.2 Off-line Measurements**

367 The off-line method was calibrated using standard solutions of H_2O_2 up to 800
368 nmol dm^{-3} . The calibration curve is shown in Figure 6. Graph (a) shows the
369 increase in fluorescence of the reaction mixture over a 15-minute period for
370 different H_2O_2 concentrations. It can be seen that the initial rate is independent
371 of the H_2O_2 concentration and after 5 – 10 minutes (depending on the H_2O_2
372 concentration) the increase in fluorescence is minimal and this is deemed to be
373 when all H_2O_2 present has reacted. A 15-minute reaction time was therefore also
374 used for the on-line instrument. Graph (b) plots the fluorescence for H_2O_2
375 standards up to 800 nmol dm^{-3} after the 15-minute reaction time when reaction
376 is complete as indicated with a dotted line in graph (a). In both graphs the blank
377 signal for the HPLC water used has been subtracted. The results indicate a

378 degree of non-linearity in the assay response in the off-line method at high H₂O₂
379 concentrations. However, in the region of interest, up to 200 – 400 nmol H₂O₂
380 dm⁻³, the relationship between H₂O₂ concentration and fluorescence intensity is
381 approximately linear. The liquid phase limit of detection is derived from the
382 variation in H₂O₂ concentrations present in the water used as a solvent.
383 Background H₂O₂ concentrations present in the water used for extraction ranged
384 from 40 – 90 nmol dm⁻³, however, on a given day the background concentrations
385 were more stable with a variation of less than ± 10 nmol H₂O₂ dm⁻³, comparable
386 to the on-line instrument. The limit of detection of particle-bound ROS (in nmol
387 m⁻³ air) is dependent on the air volume collected. Assuming a constant aerosol
388 mass concentration, the LOD decreases with increasing collection time. For a
389 one-minute filter collection (air flow: 5L min⁻¹) of oleic acid aerosol with a mass
390 concentration of 125 µg m⁻³, this equates to a detection limit of approximately
391 0.36 nmol H₂O₂ µg⁻¹. For a 10-minute filter collection, the LOD decreases to
392 0.036 nmol H₂O₂ µg⁻¹ (see discussion below for Figure 7).

393

394 For the off-line ROS quantification in oxidized oleic acid particles two filter
395 extraction methods were compared, firstly extraction by sonication and secondly
396 extraction by vortexing. Extraction by sonication for 15 minutes gave results
397 where the blank filter samples showed higher ROS concentration than the
398 sample filters on which the oxidised particles were collected. Sonication of pure
399 HPLC water gave ROS concentrations of 150 nmol dm⁻³, showing an increase of
400 80 nmol dm⁻³ compared to the same water sample before sonication, measured
401 at 70 nmol dm⁻³. The sonication of water with dissolved air present is known to
402 create hydroxyl radicals due to the high temperature and pressure created by
403 the collapse of bubbles formed by cavitation. Two hydroxyl radicals then react to
404 create H₂O₂ (Mark et al., 1998). When sample filters are sonicated, the higher
405 concentrations of soluble organics will likely scavenge hydroxyl radicals formed
406 by cavitation and thus reduce the amount of H₂O₂ produced, which might explain
407 why sonicated blank filters showed higher ROS concentrations. This emphasises
408 that sample extraction procedures should be carefully characterized when ROS
409 concentrations are determined.

410

411 As sonication itself was shown to be creating H₂O₂ during the extraction process,
412 only vortex extraction was used for the comparison of the off-line and on-line
413 method. This extraction process is still more vigorous than the process involved
414 in the on-line analysis and would be expected to result in an equally quantitative
415 extraction efficiency as the on-line method.

416

417 **3.3 Comparison of on-line versus off-line methods**

418 For a comparison of the off-line and on-line technique, measurements were performed
419 at oleic acid aerosol mass concentrations of approximately 125 µg m⁻³ which is well
420 within the linear range of both the on-line and off-line calibration curves. The
421 filter collection time was varied from 1 – 15 minutes and was repeated at least
422 three times. As the sampling time for the off-line analysis was increased, and
423 thus the delay between the start of particle collection and the addition of HRP
424 and DCFH (i.e., the start of the off-line analysis) was increased, the ROS
425 measured per particle mass decreased exponentially. In Figure 7, the
426 measurements shown by the filled black circles are taken directly after sampling,
427 the measurements shown by the open circles are for filters collected for 15
428 minutes and stored in a closed vial in the dark at room temperature for
429 approximately 7 hours and 22 hours before the remainder of the same filter was
430 extracted and analysed. When measured immediately after a short collection
431 time (1 minute), off-line measurements gave a ROS concentration of 0.75 ± 0.40
432 nmol H₂O₂ µg⁻¹ oleic acid. The relatively large error is mainly due to the very
433 short particle collection time of one minute, which inherently introduces
434 uncertainties in the total collected particle mass. However, after a 15 minute
435 sampling time ROS concentrations fell to 0.14 ± 0.05 nmol H₂O₂ µg⁻¹. When the
436 filters collected for 15 minutes were reanalysed hours later, no further decrease
437 in the ROS concentration was observed.

438

439 These off-line results can be directly compared to measurements taken using the
440 on-line instrument. The calibration curve in Figure 5 shows that a ROS
441 concentration of 0.58 nmol H₂O₂ µg⁻¹ oleic acid is measured with the on-line
442 instrument (derived from the slope of the regression analysis in Figure 5). This is

443 slightly lower but well within error limits of the shortest off-line analysis data
444 point with 0.75 ± 0.40 nmol H₂O₂ μg⁻¹ as shown in Figure 7.

445 This comparison between on-line and off-line analysis clearly shows that the
446 ROS concentration in organic particles decreases strongly within 10 – 15
447 minutes after the collection on a filter, with a major fraction of ROS having an
448 half-life of a only few minutes.

449

450 These results suggest that there are two separate types of ROS in oxidized oleic
451 acid particles: short-lived species with a half-life of a few minutes; and long-lived
452 species that are stable for hours to days. The short-lived ROS are present in
453 much higher concentrations than the long-lived ROS and could include organic
454 radical species such as the stabilised Criegee intermediate. The measured long-
455 living ROS could potentially be organic hydroperoxides.

456

457 The observed half-life of a few minutes for the short-lived species is much
458 shorter than that suggested by the only previous study aiming to estimate the
459 lifetime of ROS concentration in oxidized organic aerosols, which determined a
460 half-life of six hours (Chen et al., 2011). Our results also clearly contrast the on-
461 line/off-line comparisons of Wang et al (2011) and King and Weber (2013)
462 where comparable ROS concentrations were measured with on-line and off-line
463 methods. This discrepancy could possibly be explained by the different analysis
464 methods used and the different aerosols analysed.

465

466

467 **4 Conclusions**

468 A new instrument for on-line ROS quantification is presented and characterized.
469 One of the main differences to the only other previously described on-line ROS
470 instrument (Wang et al., 2011) is the gentle particle extraction procedure
471 applied here, which is crucial considering the reactive and short-lived nature of
472 many ROS components. The new on-line instrument has a limit of detection of
473 approximately 4 nmol H₂O₂ equivalents per m³ air and has a time resolution of

474 approximately 15 minutes. This allows following fast changing ROS
475 concentrations in the atmosphere or in laboratory studies.

476

477 For the first time we present a detailed comparison of on-line with off-line ROS
478 quantification methods using laboratory-generated oxidized oleic acid particles.
479 This comparison clearly shows that ROS in oxidized organic particles can be
480 divided into two fractions, a short-lived fraction with a half-life of only a few
481 minutes, and a long-lived ROS fraction which is stable for hours or days. The total
482 ROS concentration (in H₂O₂ equivalents) is dominated by the short-lived ROS
483 fraction, being approximately 5 times larger than the long-lived ROS
484 components. The comparison of on-line and off-line analyses presented here
485 suggests that off-line analyses methods are likely to severely underestimate
486 particle-bound ROS concentrations, and that fast on-line techniques are crucial
487 to obtain reliable, health-relevant information on ROS concentrations in
488 atmospheric aerosols.

489

490

491 **Acknowledgements**

492 This work was supported by the Natural Environment Research Council
493 (NE/H52449X/1), the Velux Stiftung (Project 593) and an ERC starting grant
494 (grant no. 279405).

495

496

497 **References**

498 Berglund, G. I., Carlsson, G. H., Smith, A. T., Szoke, H., Henriksen, A., and Hajdu, J.:
499 The catalytic pathway of horseradish peroxidase at high resolution, *Nature*, 417,
500 463-468, 2002.

501 Brunekreef, B., and Holgate, S. T.: Air pollution and health, *Lancet*, 360, 1233-
502 1242, 2002.

503 Cathcart, R., Schwieters, E., and Ames, B. N.: Detection of picomole levels of
504 hydroperoxides using a fluorescent dichlorofluorecein assay, *Analytical*
505 *Biochemistry*, 134, 111-116, 1983.

- 506 Chen, X., Hopke, P. K., and Carter, W. P. L.: Secondary Organic Aerosol from
507 Ozonolysis of Biogenic Volatile Organic Compounds: Chamber Studies of Particle
508 and Reactive Oxygen Species Formation, *Environmental Science & Technology*,
509 45, 276-282, 2011.
- 510 de Kok, T. M. C. M., Drieste, H. A. L., Hogervorst, J. G. F., and Briede, J. J.:
511 Toxicological assessment of ambient and traffic-related particulate matter: A
512 review of recent studies, *Mutation Research-Reviews in Mutation Research*, 613,
513 103-122, 2006.
- 514 Dellinger, B., Pryor, W. A., Cueto, R., Squadrito, G. L., Hegde, V., and Deutsch, W. A.:
515 Role of free radicals in the toxicity of airborne fine particulate matter, *Chemical*
516 *Research in Toxicology*, 14, 1371-1377, 2001.
- 517 Dockery, D. W., Pope, C. A., Xu, X. P., Spengler, J. D., Ware, J. H., Fay, M. E., Ferris, B.
518 G., and Speizer, F. E.: An association between air-pollution and mortality in 6
519 United-States cities, *New England Journal of Medicine*, 329, 1753-1759, 1993.
- 520 Donaldson, K., Stone, V., Borm, P. J. A., Jimenez, L. A., Gilmour, P. S., Schins, R. P. F.,
521 Knaapen, A. M., Rahman, I., Faux, S. P., Brown, D. M., and MacNee, W.: Oxidative
522 stress and calcium signaling in the adverse effects of environmental particles
523 (PM₁₀), *Free Radical Biology and Medicine*, 34, 1369-1382, 2003.
- 524 Gerlofs-Nijland, M.E., Dormans, J.A.M.A., Bloemen, H.J.T., Leseman, D.L.A.C., Boere,
525 A.J.F., Kelly, F.J., Mudway, I.S., Jimenez, A.A., Donaldson, K., Guastadisegni, C.,
526 Janssen, N.A.H., Brunekreef, B., Sandstrom, T., Cassee, F.R.: Toxicity of coarse and
527 fine particulate matter from sites with contrasting traffic profiles, *Inhalation*
528 *Toxicology*, 19, 1055-1069, 2007.
- 529 Halliwell, B., and Gutteridge, J.: *Free Radicals in Biology and Medicine*. Oxford
530 University Press, 2007.
- 531 Hasson, A. S., Orzechowska, G., and Paulson, S. E.: Production of stabilized Criegee
532 intermediates and peroxides in the gas phase ozonolysis of alkenes 1. Ethene,
533 trans-2-butene, and 2,3-dimethyl-2-butene, *Journal of Geophysical Research-*
534 *Atmospheres*, 106, 34131-34142, 2001.
- 535 Hung, H. F., and Wang, C. S.: Experimental determination of reactive oxygen
536 species in Taipei aerosols, *Journal of Aerosol Science*, 32, 1201-1211, 2001.
- 537 Hwang, H., and Dasgupta, P. K.: Fluorometric flow-injection determination of
538 aqueous peroxides at nanomolar level using membrane reactors, *Analytical*
539 *Chemistry*, 58, 1521-1524, 1986.
- 540 Katrib, Y., Martin, S. T., Rudich, Y., Davidovits, P., Jayne, J. T., and Worsnop, D. R.:
541 Density changes of aerosol particles as a result of chemical reaction, *Atmospheric*
542 *Chemistry and Physics*, 5, 275-291, 2005.
- 543 King, L. E., and Weber, R. J.: Development and testing of an online method to
544 measure ambient fine particulate Reactive Oxygen Species (ROS) based on the
545 2',7'-dichlorofluorescein (DCFH) assay, *Atmos. Meas. Tech.*, 6, 1647 - 1658, 2013.

546 MacNee, W., and Donaldson, K.: Mechanism of lung injury caused by PM10 and
547 ultrafine particles with special referance to COPD, *European Respiratory Journal*,
548 21, 47S-51S, 2003.

549 Mark, G., Tauber, A., Rudiger, L. A., Schuchmann, H. P., Schulz, D., Mues, A., and
550 von Sonntag, C.: OH-radical formation by ultrasound in aqueous solution - Part II:
551 Terephthalate and Fricke dosimetry and the influence of various conditions on
552 the sonolytic yield, *Ultrasonics Sonochemistry*, 5, 41-52, 1998.

553 Orsini, D. A., Ma, Y. L., Sullivan, A., Sierau, B., Baumann, K., and Weber, R. J.:
554 Refinements to the particle-into-liquid sampler (PILS) for ground and airborne
555 measurements of water soluble aerosol composition, *Atmospheric Environment*,
556 37, 1243-1259, 2003.

557 Pryor, W. A., and Church, D. F.: Aldehydes, hydrogen-peroxide, and organic
558 radicals as mediators of ozone toxicity, *Free Radical Biology and Medicine*, 11,
559 41-46, 1991.

560 Takeuchi, M., Ullah, S. M., Dasgupta, P. K., Collins, D. R., and Williams, A.:
561 Continuous collection of soluble atmospheric particles with a wetted hydrophilic
562 filter, *Anal Chem*, 77, 8031-8040, 2005.

563 Venkatachari, P., and Hopke, P. K.: Development and laboratory testing of an
564 automated monitor for the measurement of atmospheric particle-bound reactive
565 oxygen species (ROS), *Aerosol Science and Technology*, 42, 629-635, 2008.

566 Venkatachari, P., Hopke, P. K., Grover, B. D., and Eatough, D. J.: Measurement of
567 particle-bound reactive oxygen species in Rubidoux aerosols, *Journal of*
568 *Atmospheric Chemistry*, 50, 49-58, 2005.

569 Vesna, O., Sax, M., Kalberer, M., Gaschen, A., Ammann, M.: Product Study of Oleic
570 Acid Ozonolysis as Function of Humidity, *Atmos. Environ.*, 43, 3662-3669, 2009.

571 Wang, Y., Arellanes, C., and Paulson, S. E.: Hydrogen Peroxide Associated with
572 Ambient Fine-Mode, Diesel, and Biodiesel Aerosol Particles in Southern
573 California, *Aerosol Science and Technology*, 46, 394-402, 2012.

574 Wang, Y., Hopke, P. K., Sun, L., Chalupa, D. C., and Utell, M. J.: Laboratory and field
575 testing of an automated atmospheric particle-bound reactive oxygen species
576 sampling-analysis system, *Journal of toxicology*, 2011, 419476, 2011.

577 Ziemann, P. J.: Aerosol products, mechanisms, and kinetics of heterogeneous
578 reactions of ozone with oleic acid in pure and mixed particles, *Faraday*
579 *Discussions*, 130, 469-490, 2005.

580
581
582
583
584
585
586

587 **Figure Captions**

588

589 **Figure 1.** The reaction scheme of DCFH/HRP with peroxides (a) demonstrating
590 the initial reaction of ROS (H_2O_2) with HRP, followed by reaction with DCFH to
591 form the fluorescent product DCF. The reaction of HRP with oxygen (b) also
592 leads to the formation of DCF and is accounted for in blank measurements
593 (schematic modified after Berglund et al., 2002).

594

595 **Figure 2.** Schematic of the oxidised oleic acid aerosol generation system where
596 oleic acid aerosol is produced through heating and reacted with ozone before
597 passing through a charcoal denuder to remove organic gas phase products and
598 excess ozone. The number size distribution of the aerosol particles is measured
599 using an SMPS in parallel to particle-bound ROS concentration measurements.

600

601 **Figure 3.** Schematic of the on-line particle-bound ROS measurement instrument.
602 Particles are collected on hydrophilic filters in the small particle collector (150
603 mm height, 30 mm diameter) and soluble components are extracted for on-line
604 analysis using the DCFH/HRP-fluorescence assay.

605

606 **Figure 4.** Calibration of on-line instrument with hydrogen peroxide, showing a
607 linear relationship to fluorescence intensity and an LOD of approximately 10
608 nmol $\text{H}_2\text{O}_2 \text{ dm}^{-3}$. Error bars are smaller than the symbol size and thus are not
609 visible.

610

611 **Figure 5.** Results of the on-line instrument showing measured ROS
612 concentrations versus oxidised oleic aerosol mass concentrations. This strong
613 linear relationship shows that the aerosol generated has a consistent ROS
614 concentration per particle mass. Measurements were performed during three
615 days demonstrating the reproducibility of the ROS generation using oxidized
616 oleic acid. Each symbol (squares, circles and diamonds) represents the
617 measurements taken during one of the three days.

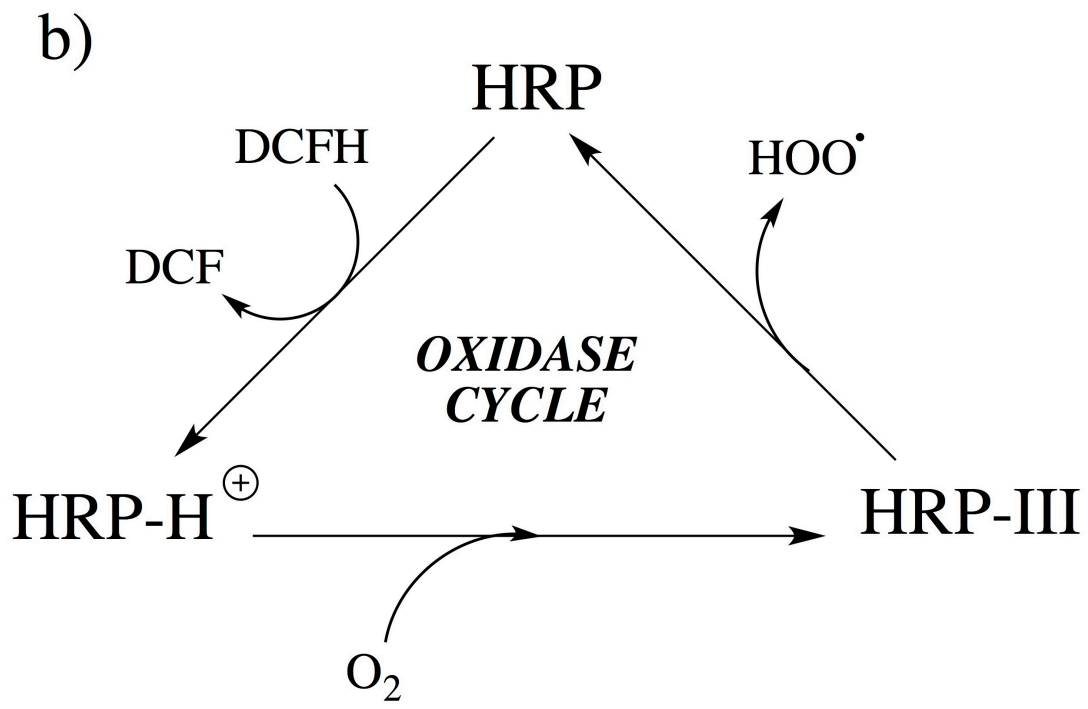
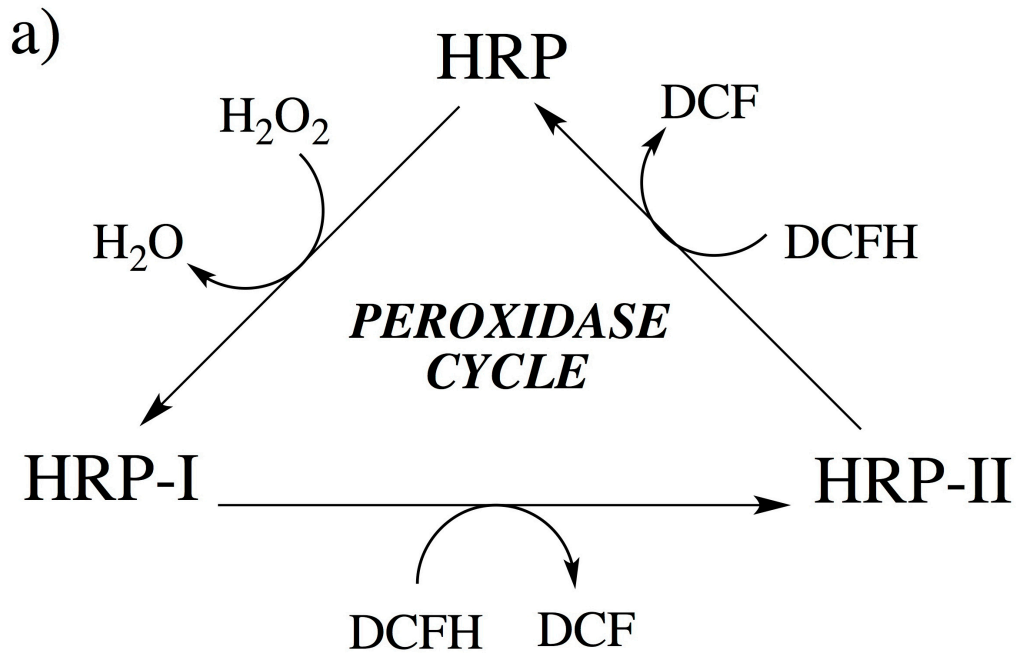
618

619 **Figure 6.** Calibration of off-line method with hydrogen peroxide showing the
620 increase in fluorescence intensity with time for a range of hydrogen peroxide
621 concentrations (a) and the end-point fluorescence intensity after 15 minutes
622 against H_2O_2 concentration (b).

623

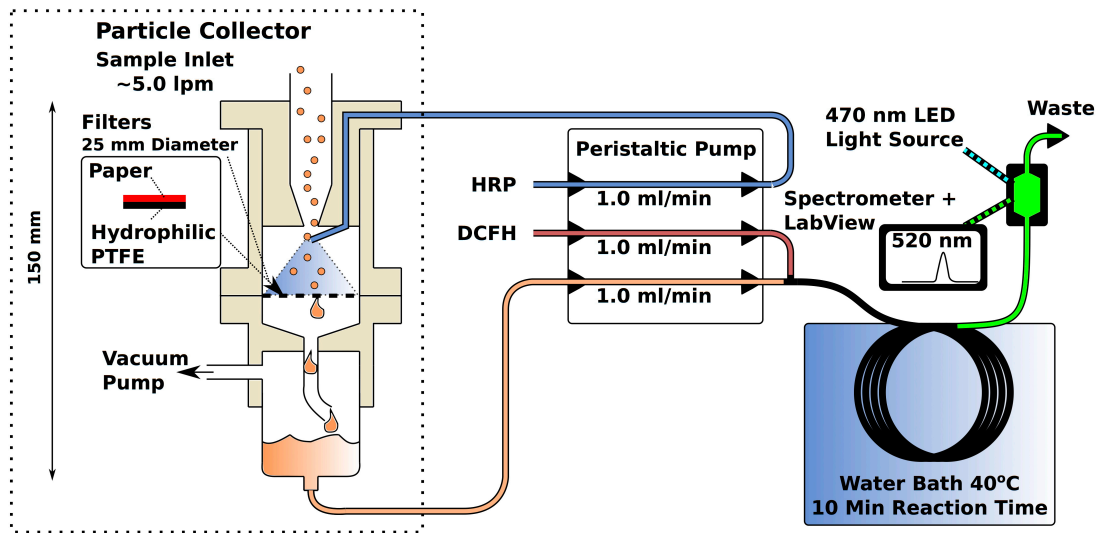
624 **Figure 7.** Comparison of ROS concentrations in oxidized oleic acid particles
625 using the on-line instrument and the off-line method. Results from the off-line
626 method show a strong decrease in ROS concentration with increased time
627 between filter sampling and analysis, which levels off after ~15 minutes (filled
628 and empty circles). The limit of detection for the off-line method is indicated by
629 the grey striped line. ROS concentrations quantified with the on-line instrument
630 are shown for comparison (diamond symbol) and are comparable with the off-
631 line method only for samples with the shortest collection time (one minute).

632



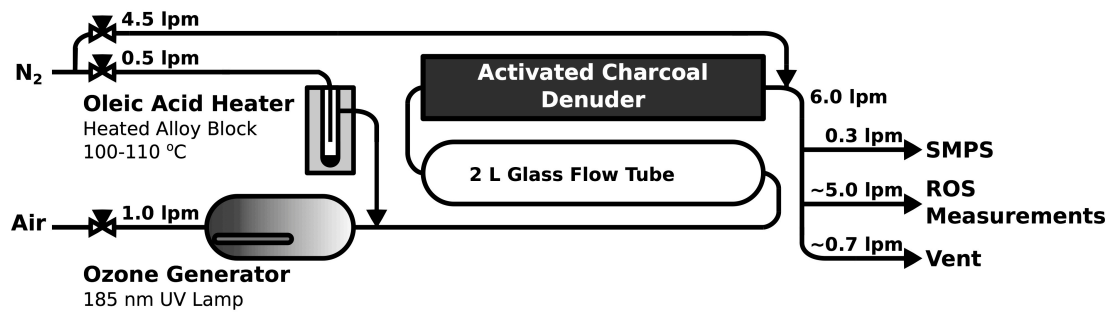
633
634
635
636

Figure 1



637
638
639
640

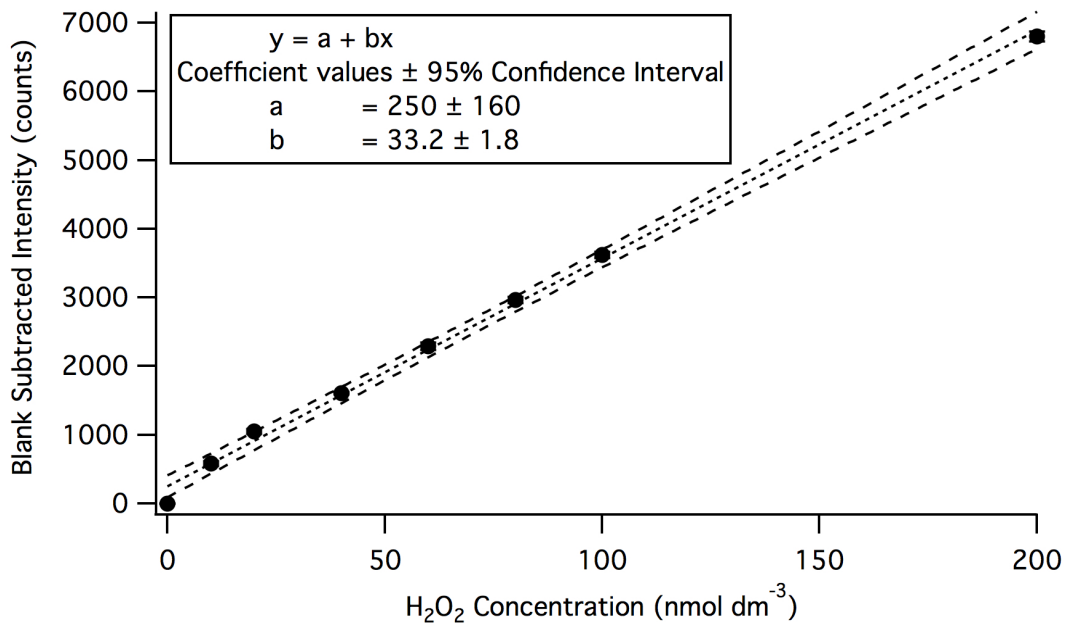
Figure 2



641
642
643
644

Figure 3

645



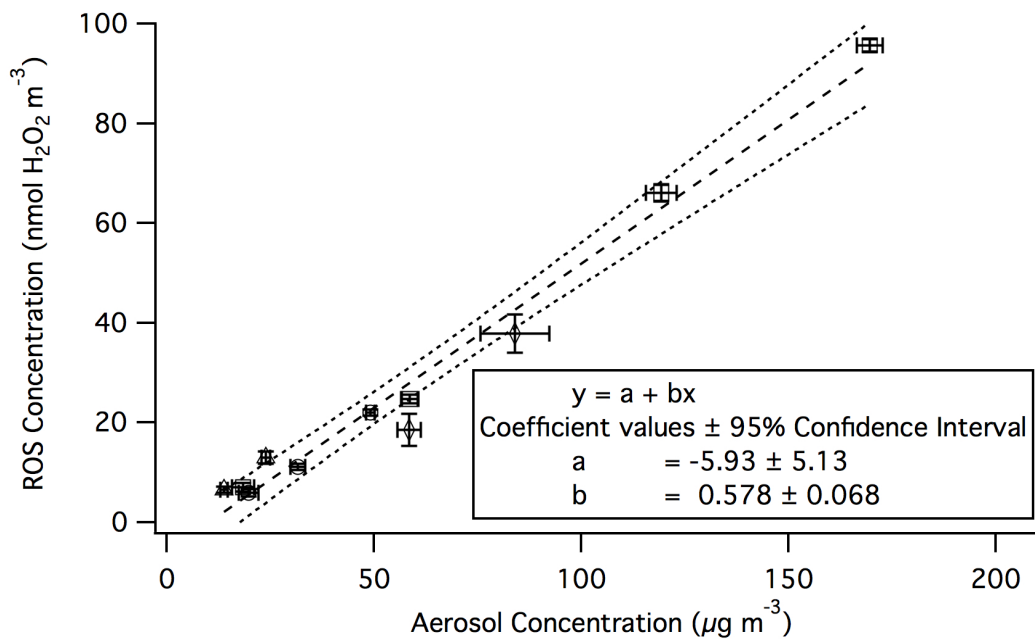
646

647

648

649

Figure 4



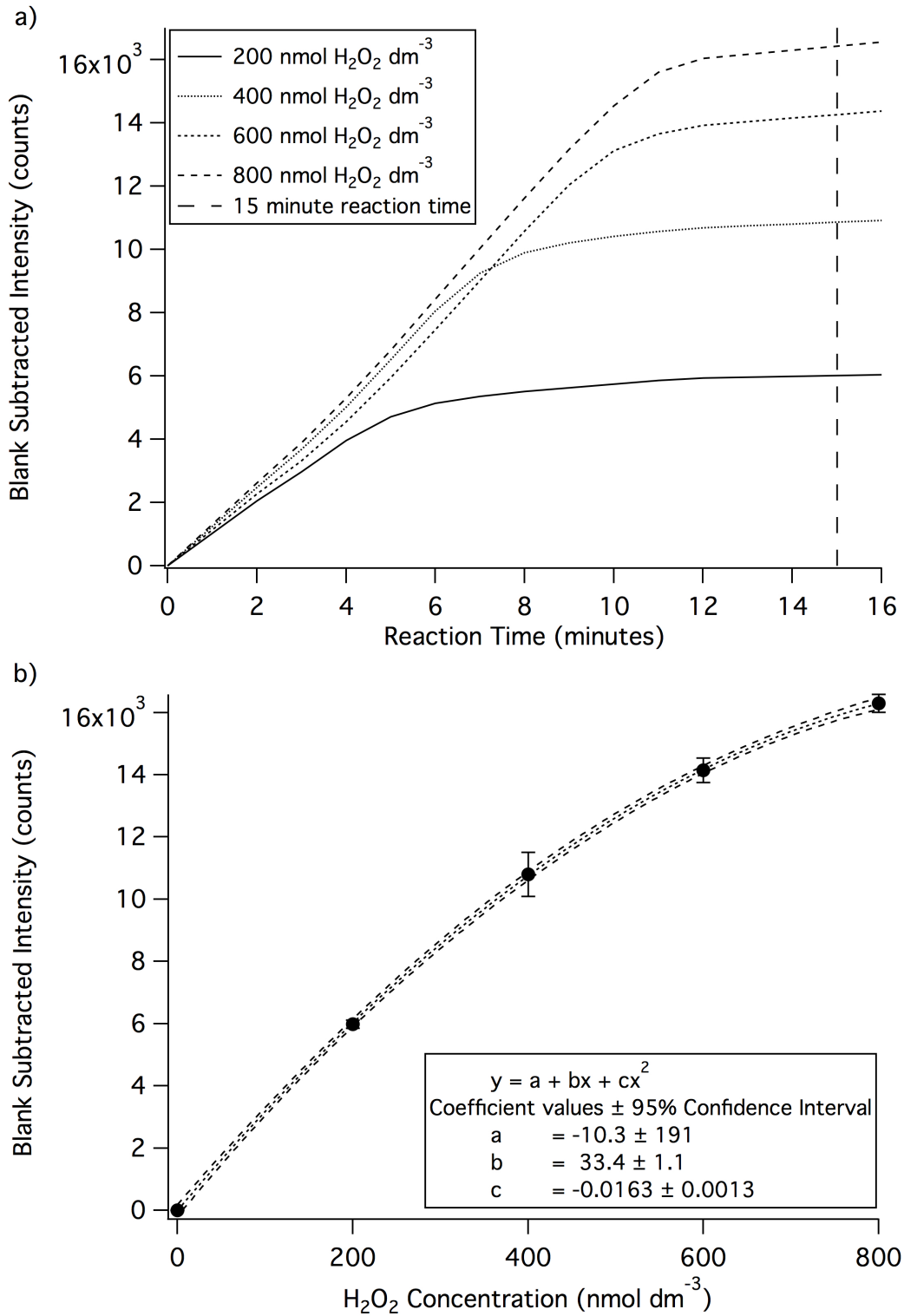
650

651

652

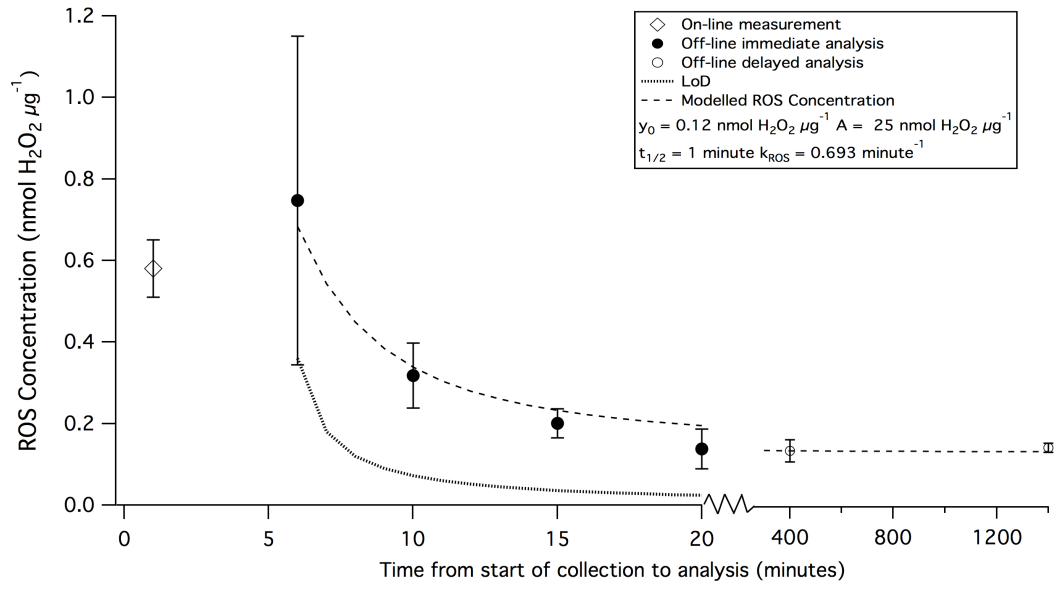
653

Figure 5



654
 655
 656

Figure 6



657
 658
 659

Figure 7